Shared Components of the FRQ-Less Oscillator and TOR Pathway Maintain Rhythmicity in *Neurospora*

Rosa Eskandari (iD), Lalanthi Ratnayake and Patricia L. Lakin-Thomas[1] (iD)

Department of Biology, York University, Toronto, ON, Canada

Abstract   Molecular models for the endogenous oscillators that drive circadian rhythms in eukaryotes center on rhythmic transcription/translation of a small number of "clock genes." Although substantial evidence supports the concept that negative and positive transcription/translation feedback loops (TTFLs) are responsible for regulating the expression of these clock genes, certain rhythms in the filamentous fungus *Neurospora crassa* continue even when clock genes (*frq*, *wc-1*, and *wc-2*) are not rhythmically expressed. Identification of the rhythmic processes operating outside of the TTFL has been a major unresolved area in circadian biology. Our lab previously identified a mutation (*vta*) that abolishes FRQ-less rhythmicity of the conidiation rhythm and also affects rhythmicity when FRQ is functional. Further studies identified the *vta* gene product as a component of the TOR (Target of Rapamycin) nutrient-sensing pathway that is conserved in eukaryotes. We now report the discovery of TOR pathway components including GTR2 (homologous to the yeast protein Gtr2, and RAG C/D in mammals) as binding partners of VTA through co-immunoprecipitation (IP) and mass spectrometry analysis using a VTA-FLAG strain. Reciprocal IP with GTR2-FLAG found VTA as a binding partner. A Δ*gtr2* strain was deficient in growth responses to amino acids. Free-running conidiation rhythms in a FRQ-less strain were abolished in Δ*gtr2*. Entrainment of a FRQ-less strain to cycles of heat pulses demonstrated that Δ*gtr2* is defective in entrainment. In all of these assays, Δ*gtr2* is similar to Δ*vta*. In addition, expression of GTR2 protein was found to be rhythmic across two circadian cycles, and functional VTA was required for GTR2 rhythmicity. FRQ protein exhibited the expected rhythm in the presence of GTR2 but the rhythmic level of FRQ dampened in the absence of GTR2. These results establish association of VTA with GTR2, and their role in maintaining functional circadian rhythms through the TOR pathway.

Keywords   FRQ-less oscillator, circadian rhythm, FRQ, Ragulator, TOR pathway

---

1. To whom all correspondence should be addressed: Patricia L. Lakin-Thomas, Department of Biology, York University, 4700 Keele Street, Toronto M3J 1P3, ON, Canada; e-mail: plakin@yorku.ca.

Molecular oscillators responsible for circadian rhythmicity in eukaryotes are supported by the rhythmic transcription of clock genes. Rhythmic transcription and translation of clock genes as a result of positive and negative feedback loops form the core of molecular models known as transcription/translation feedback loops (TTFLs).

Although substantial evidence provides support for the concept of a key role for negative and positive TTFLs in regulating the expression of clock genes, the TTFL model is inadequate to completely explain the clock mechanism. It has been observed that certain rhythms in various organisms continue even when clock genes are not rhythmically expressed, or are nonfunctional (Bass, 2012; Lakin-Thomas, 2006b, 2019; van Ooijen and Millar, 2012). In cyanobacteria, a circadian rhythm of protein phosphorylation can be sustained in a test tube with a limited number of components (Nakajima et al., 2005; Tseng et al., 2017). This rhythmic process has been well-studied in the bacterial system. However, in eukaryotes, identification of the rhythmic processes operating outside of TTFLs has been a major unresolved area in circadian biology that is relevant to all eukaryotic cells. Further advancement in the understanding of circadian oscillators in eukaryotes is dependent on the identification of clock components outside of the TTFL.

Many researchers have contributed to our understanding of the molecular basis of circadian rhythmicity by investigating the filamentous fungus *Neurospora crassa* as a model organism. The current model for the *Neurospora* circadian oscillator (also known as the FRQ/WCC TTFL) consists of interlocked negative and positive transcription/translation feedback loops comprising the clock genes *frq*, *wc-1*, and *wc-2*. Although the majority of investigations on the *Neurospora* circadian system are dedicated to the FRQ/WCC feedback loop, it has been well known for many years that rhythmic conidiation can be observed in the absence of a functional *frq* gene (Lakin-Thomas et al., 2011; Ratnayake et al., 2018). In our lab we use two assay systems to reveal FRQ-less rhythms: first, in the choline-requiring *chol-1* strains, the period of rhythmicity depends on the concentration of choline in the medium and this rhythmicity persists in FRQ-less strains as well (Lakin-Thomas and Brody, 2000); second, entrainment of FRQ-less strains to cycles of heat pulses shows the characteristics of an internal oscillator (Lakin-Thomas, 2006a). An oscillator must drive rhythmicity in the absence of the functions of FRQ/WCC, and our research is focused on identifying the components of the FRQ-less oscillator(s) (FLOs) and investigating the relationship between the FRQ/WCC and the FLO.

In order to identify genes required to maintain FRQ-less rhythmicity, we carried out a mutagenesis screen in a FRQ-less strain (Li et al., 2011). We identified a mutation (temporarily named uv90) that disrupts the conidiation rhythm in FRQ-less strains under our two different assay systems: rhythmic entrainment to short heat pulses and free-running rhythmicity in *chol-1* strains deprived of choline. In the FRQ wild-type background, this mutation reduces the amplitude of the FRQ protein rhythm and dampens the rhythm of conidiation. We demonstrated that this mutation dampens the amplitude of the entire circadian oscillator in the FRQ wild-type background, as evaluated by the response to phase resetting by light or heat pulses. Therefore, the uv90 mutation identifies a gene that is required for robust FRQ-less rhythmicity and also for maintaining the amplitude of the entire circadian system in the presence of FRQ.

We subsequently mapped the uv90 mutation and identified the gene as NCU05950 (Ratnayake et al., 2018). We identified the gene product as a component of the TOR (Target of Rapamycin) pathway, according to three criteria:

1. The uv90 gene sequence is similar to p18/LAMTOR1 in mammals and EGO1/Meh1p/Gse2p in yeast. These proteins are found on lysosomal/vacuolar membranes and are responsible for anchoring protein complexes that function to activate TOR in response to nutritional signals, specifically amino acids. Activation of TOR in yeast and mammals leads to increased cellular growth.
2. The uv90 protein product localizes to the outer vacuolar membrane, as predicted by sequence analysis. We also found that this localization is required for the clock-related function of the uv90 protein product.
3. A uv90 knockout fails to increase growth in response to amino acid supplementation, as predicted by its similarity to homologous proteins in yeast and mammals.

We therefore renamed the uv90 gene *vta* and the protein product VTA, for "vacuolar TOR-associated protein" (Ratnayake et al., 2018).

The mechanistic TOR is a Serine/Threonine kinase, which consists of two separate complexes in mammals (mTOR) and yeast (TOR). TOR kinases are found in all domains of eukaryotic life. The primary function of the TOR signaling pathway is to integrate nutritional as well as growth signals and coordinate their effects at the cellular level. Activation of this pathway will lead to an increase in
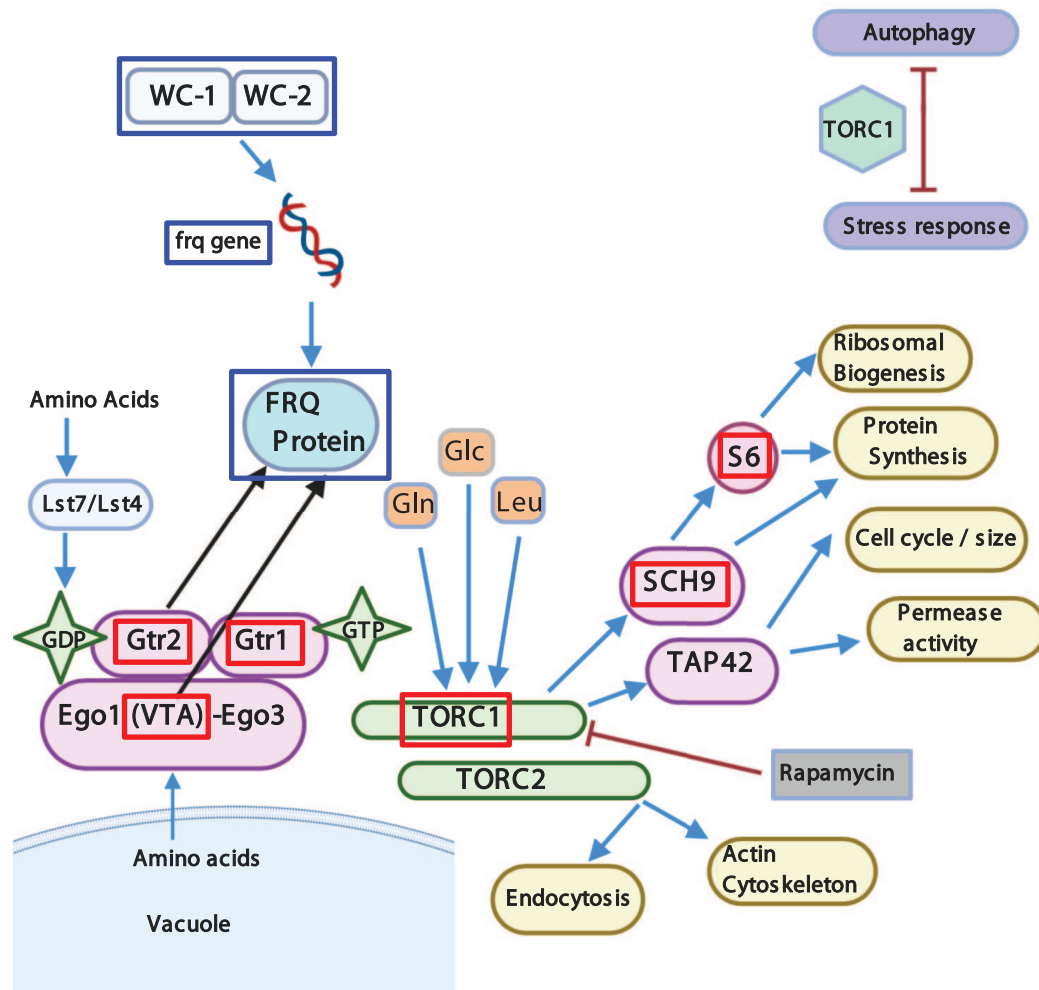
Figure 1.   The TOR pathway as described in budding yeast (González and Hall, 2017; Loewith and Hall, 2011; Saxton and Sabatini, 2017). Blue arrows show activation, red blunt-end lines show inhibition. Gln, Leu, Glc: glutamine, leucine, glucose. *Neurospora* proteins identified as probable components of the TOR pathway are outlined in red boxes. Blue boxes outline *Neurospora* clock proteins WC-1, WC-2, and FRQ (not found in yeast). Black arrows suggest an influence of VTA and GTR2 on FRQ protein in *Neurospora*. Created with BioRender.com.

anabolic processes and a decrease in catabolic processes (Boutouja et al., 2019).

The TOR pathway has been intensively studied in yeast and mammals. In *Saccharomyces cerevisiae* (Figure 1), two multi-protein complexes have been identified (Loewith and Hall, 2011). TORC1, which is rapamycin sensitive and is located on the vacuolar membrane, is responsive to nutrient signals and controls a wide-ranging variety of readouts including protein synthesis and degradation, messenger RNA (mRNA) synthesis and degradation, ribosome biogenesis, nutrient uptake, and autophagy. TORC2 controls the polarized organization of the actin cytoskeleton, endocytosis, and sphingolipid synthesis (Loewith and Hall, 2011).

The EGO complex is an important regulator of TORC1 in yeast, which consists of Ego1, Ego2, Ego3, Gtr1, and Gtr2 (Powis et al., 2015). Gtr1 and Gtr2 are Ras-family GTPases and homologs of the metazoan Rag GTPases. Ego1 and Ego3 are homologs of the vertebrate proteins p18 (LAMTOR1) and P14+MP1 (LAMTOR2+LAMTOR3). In yeast, the EGO complex localizes to the vacuolar membrane and responds to intra-vacuolar amino acid levels. The $Gtr1^{GTP} Gtr2^{GDP}$ combination activates TORC1, and activated TORC1 phosphorylates and activates Sch9, which is homologous to S6 kinase in mammals. TORC1 also regulates phosphatases in yeast through regulatory protein Tap42. Inactivation of TORC1 results in Tap42 dephosphorylation and a weak association with

phosphatases that results in their activation or change in substrate preference (Loewith and Hall, 2011).

In mammals, extracellular growth factors produce their effects by using cell-surface receptors to activate the kinase AKT and the tuberous sclerosis complex (TSC), which in turn leads to the activation of mTORC1. The mTORC1 complex is also activated by amino acids by poorly characterized pathways that are not dependent on the cell-surface receptors and the TSC. The Ragulator-Rag GTPase complex (p18/LAMTOR1, p14/LAMTOR2, MP1/LAMTOR3, p10/LAMTOR4/C7orf59, HBXIP/LAMTOR5, RagA/B, and RagC/D) mediates amino acid sufficiency signals to mTORC1 (Yonehara et al., 2017). Activation of mTORC1 leads to the phosphorylation of substrates including S6K, which further leads to the phosphorylation of the ribosomal protein S6. mTORC1 also phosphorylates translation inhibitor 4E-BP, which then leads to the release of eIF4E to increase translation (Jewell et al., 2013). It has been observed that in both mammals and yeast, localization of the TOR complex to the lysosomal/vacuolar membrane is required for its activation (Sancak et al., 2010).

Our current research continues our effort to identify components of the FLO, and to expand our understanding of the function of VTA and its role in the *Neurospora* TOR pathway. Our immediate goal was to answer the question: Do other components of the TOR pathway in *Neurospora* also influence the circadian system?

Although the TOR pathway has been well-studied in yeast, very little is known about the components of this pathway in filamentous fungi such as *Neurospora*. Genomic analyses have identified highly conserved putative TOR pathway genes in the fungal kingdom (Shertz et al., 2010) but there are few functional studies. Rapamycin (or FK506) binding proteins (FKBPs) have been studied in *Neurospora* (Pinto et al., 2008). A survey of knockouts of putative Ser/Thr kinase genes in *Neurospora* (Park et al., 2011) identified STK-10 as a homolog of the TOR substrate Sch9/S6K and found that the knockout showed impaired growth and osmoregulation. A homolog of the TORC1/TORC2 kinase was identified in this study but no phenotypic analysis was carried out (Park et al., 2011). Other components of the TOR signaling pathway, in particular potential components of an EGO or Ragulator complex, have not been described beyond our identification of VTA. We therefore began our investigation by looking for binding partners of VTA that are likely to be components of the *Neurospora* homolog to the yeast/mammalian EGO/Ragulator complexes.

We have now identified *Neurospora* gene NCU00376 as a homolog of yeast Gtr2 and mammalian Rag C/D, by the criteria of co-precipitation with VTA, sequence similarity, and requirement of the gene product for normal growth response to amino acid supplementation. We have found that the rhythmic phenotype of the NCU00376 (*gtr2*) knockout is very similar to that of the VTA knockout, in that it disrupts FRQ-less conidiation rhythmicity in two different assay systems and damps conidiation rhythmicity in the presence of FRQ. As with VTA, the knockout also damps the rhythm of FRQ protein expression. We therefore conclude that the protein product GTR2 is another TOR pathway component in *Neurospora* that plays an important role in maintaining circadian rhythmicity in both FRQ-sufficient and FRQ-deficient backgrounds.

MATERIALS AND METHODS

Strains

The Oak Ridge (OR) strain (FGSC #4200) was obtained from the Fungal Genetics Stock Center (FGSC, Kansas State University, Manhattan, KS; McCluskey et al., 2010). Δ*vta* (FGSC #18029) and Δ*gtr2* (FGSC #16041) strains produced by the *Neurospora* Functional Genomics Project (Dunlap et al., 2006) were also obtained from FGSC and were crossed into our lab strains by standard crossing techniques (Lakin-Thomas and Brody, 2000). GTR2-FLAG strains were constructed in our laboratory using the homologous recombination system in yeast and by LiAc-mediated yeast transformation techniques (Honda and Selker, 2009), as described below. All strains carry the *ras^{bd}* mutation, which prevents conidiation suppression in response to the accumulation of CO_2 in closed race tubes. The *chol-1* mutation impairs synthesis of the lipid phosphatidylcholine. The *chol-1* mutant strains require choline supplementation for normal growth as well as normal rhythmicity and with choline supplementation they are indistinguishable from *chol^+* strains. This allows us to assay FRQ-less rhythms that do not depend on choline depletion, such as heat pulse entrainment behavior. The *csp-1* mutation prevents the separation of conidiospores from aerial hyphae (Ratnayake et al., 2018).

Construction of GTR2-FLAG

A 1.1 kb fragment including the 3′-end of the GTR2 (NCU00376) coding region, without the stop codon, was amplified from the genomic DNA of a *csp-1*; *chol-1 ras^{bd}* strain using the following forward primer: <u>GTAACGCCAGGGTTTTCCCAGTCACGACGCC</u>TTCATTCTACCCTCATAC, which contains 29 nt of homology (indicated by underlining) at one end of the linearized pRS426 (shuttle vector, obtained from

FGSC), and reverse primer: <u>CCTCCGCCTCCGCCT CCGCCGCCTCCGCC</u>ACGACCATCACCCACCA CCC, which contains 29 nt of homology at the 5′-end of the 3xFLAG knock-in module. A 500 bp fragment of the 3′ GTR2 flanking region was amplified with the forward primer: <u>TGCTATACGAAGTTATGGATCCG AGCTCG</u>GGATTTCATCCGGTTGTTTG, which contains 29 nt of homology with the 3′-end of the 3xFLAG knock-in module, and reverse primer: <u>GCGGATAA C A A T T T C A C A C A G G A A A C A G C C</u> A C C CAGCCAACCAAGTACC, which contains 29 nt of homology at the other end of the linearized pRS426. pRS426 was linearized by digestion with Xhol-1 and EcoRI, and a 3xFLAG knock-in module (3xFLAG::loxP::hph::loxP) was isolated from p3xFLAG::hph::loxP (FGSC) by digestion with KpnI and XhoI. The yeast strain FY834 was co-transformed with linearized pRS426, the 3xFLAG knock-in module, and the two polymerase chain reaction (PCR) products for assembly in yeast by using its endogenous homologous recombination system and using the LiAc-mediated yeast transformation method (Oldenburg et al., 1997). Yeast colonies were picked using SC media without uracil, and the presence of the correct cassette was confirmed by colony PCR with the 5′ forward and 3′ reverse GTR2-FLAG cassette-specific primers. DNA was extracted from the yeast colonies that contained the correct cassette by using a plasmid extraction kit (FroggaBio, Concord, ON, Canada). DNA was then transformed into *Escherichia coli* competent cells (New England BioLabs, Ipswich, MA), and after extracting the plasmids from bacterial colonies, the final bacterial plasmid carrying the correct cassette was confirmed by restriction enzyme digestion and sequencing. The cassette was then amplified by using 5′ forward and 3′ reverse primers specific for both sides of the cassette, and the cassette was then transformed by electroporation into the *mus-51 his-3* strain of *N. crassa* deficient in non-homologous end joining (Honda and Selker, 2009). Transformation mixture was plated on agar plates (0.1% fructose, 0.1% glucose, 2% sorbose, 1× Vogel's salt, 2% agar, 25 mg/mL histidine) with hygromycin B (200 μg/mL; BioShop, Burlington, Ontario, Canada), as a selectable marker. Transformed colonies were picked and grown on slants containing Vogel's minimal media including histidine (25 mg/mL) and choline (2 mg/mL) as supplements and hygromycin as a selection agent. Slants were left at 30 °C for 7 days. To confirm the presence of the cassette, spores were genotyped using Terra PCR Direct kit (Takara Bio, Mountain View, CA), and *gtr2*-specific primers. Heterokaryon strains (with two different alleles of the *gtr2* gene) were crossed into our lab strains. After 4 weeks, ascospores from the cross between GTR2-FLAG (*mus51*, *his-3*) and *csp-1*; *chol-1* *ras^{bd}*; Δ*vta*; *frq^{10}* were heat-shocked and plated on

sorbose plating media. Colonies appeared after 1-3 days and were then picked and grown in new slants containing appropriate supplements and were left in 30 °C for 7 days. Slant cultures were genotyped for the presence/absence of *csp-1*, *chol-1*, *ras^{bd}*, *mus-51*, *vta*, *frq^{10}* and GTR2-FLAG cassette, by PCR and restriction enzyme digestion. Final candidates were then inoculated on race tubes for period and growth phenotype analysis.

To ensure the normal expression of the GTR2-FLAG protein, immunoblotting was carried out with anti-FLAG antibodies. A strain without any FLAG (*csp-1*; *chol-1* *ras^{bd}*) was used as the negative control. The FLAG-tagged GTR2 protein demonstrated expression in the expected region (48 KD) and no band was observed in the negative control lane (data not shown).

Race Tube Analysis of Clock Phenotypes

For assaying rhythmicity of conidiation, cultures were inoculated from conidiospores and were grown on solid agar medium in long glass growth tubes ("race tubes") on media containing 1× Vogel's salts, 0.5% maltose, 0.01% arginine, and 2% agar, in the presence or absence of choline (100 μM). Race tubes were kept in LL (constant light) at 30 °C for 1 day before transfer to 22 °C DD (constant dark), and the growth front was marked once a day. Period and growth rate were calculated using in-house software as previously described (Adhvaryu et al., 2016). Mean periods were compared by unpaired two-tailed Student's *t* tests using Prism GraphPad.

Entrainment to Heat Pulses

Cultures were grown as for race tube analysis, except after an initial day at 30 °C in LL tubes were subjected to a heat pulse for 2 h at 32 °C in DD followed by 22 °C in DD for 18 h or 22 h. Heat pulses were repeated at intervals of T = 20 h or T = 24 h. After growth had finished, the patterns of conidial density were analyzed as previously described (Adhvaryu et al., 2016; Lakin-Thomas, 2006a; Li and Lakin-Thomas, 2010). Race tubes were scanned and the density analyzed by PlotProfile in Fiji (ImageJ) software (http://fiji.sc). The density profiles were corrected for growth rate, binned into 0.1 h bins, and averaged over 4-6 replicate race tubes. One or two T-cycles were chosen after the cultures had reached stable entrainment, shown by peaks in the control strain at approximately the same time in most replicate race tubes and at the same time in subsequent cycles. For T = 20 h, the third and fourth cycles were averaged for Δ*frq* Δ*vta* and Δ*frq* Δ*gtr2* and the fourth cycle was used for Δ*frq*. For T = 24, the fifth and sixth

cycles were used for all strains. Mean density and SEM were calculated for the average cycle for each set of replicate tubes and the density was normalized to peak value = 1.0. For smoothed density profiles, a 19-point running average (equivalent to a 1.9 h moving window) was calculated and plotted at the midpoint of the 19-point window.

Growth Rate Assay in Liquid Media

Conidiospores from fresh cultures of Δ*gtr2* and Oak Ridge wild-type strains were counted in a hemocytometer, and 1000 spores per 1 mL of liquid minimal media were aliquoted into 24-well plates and incubated for 48 h at 25 °C in a 12:12 L:D cycle. Media contained 1× Vogel's salts and varying concentrations of glucose, or 1× Vogel's salts, 2% glucose, and amino acids (5 mM) with or without the standard Vogel's nitrogen source NH_4NO_3. The mycelial mats were harvested and washed with water 3 times over nylon net filters, placed in pre-weighed aluminum foil boats and dried at 80 °C for 48 h. The dry weight of the samples was calculated as the difference between the weights of the foil with and without the fungus. Three replicates of each condition were averaged to give one value for each independent experiment, and weights were normalized within each experiment by setting wild type on VM + 2% glucose equal to 1.0. The mean was then calculated from three or four independent experiments. In each independent experiment, the Δ*gtr2* strain was compared to the wild type in a paired design. Means were compared by paired two-tailed Student's *t* test using Prism GraphPad.

Time-course Experiments and Immunoblotting

To investigate the relative amounts of GTR2 or FRQ protein across the circadian cycle, time-course experiments were conducted as previously described (Li et al., 2010). Spores were inoculated on starter plates containing 1× Vogel's salts, 0.5% maltose, 0.01% arginine, 2% agar, and 100 µM choline and incubated in LL at 30 °C. After several days of growth, plugs of mycelium were removed from the growth front by punching using sterile glass pipettes and plugs were inoculated on the top of cellophane layered over plates containing the same medium. Plates were incubated at 30 °C in LL, then transferred to 22 °C in DD at various times and harvested after 48-76 h of total growth. The times of transfer to DD were varied so that total hours in DD varied from 24 to 72 h. Samples were harvested from one centimeter of the growth front and were immediately frozen in liquid nitrogen and stored at −80 °C until protein extraction. Three independent time-courses were carried out for each strain.

Protein extraction was conducted by grinding the frozen fungal mycelium in liquid nitrogen with a mortar and pestle. Powdered mycelium was then added to a microfuge tube containing 200 µL of protein extraction buffer (PEB) (50 mM tris pH 6.8, 2% sodium dodecyl (lauryl) sulfate [SDS], 10% glycerol, 5 mM ethylenediaminetetraacetic acid [EDTA], 1 mM phenylmethylsulfonyl fluoride [PMSF]), vortexed and boiled for 5 min immediately and left on ice. After extraction, all samples were centrifuged for 5 min at 12,000×*g* at 25 °C. Protein concentration was then assayed using Bio-Rad DC Protein Assay (Bio-Rad Laboratories, Mississauga, Ontario, Canada). Thereafter, a total volume of 20 µL of the protein samples in PEB buffer containing 20 µg of total protein, 1 µL of 1% bromophenol blue and 1/10 volume of 0.1 M dithiothreitol was boiled for 2 min and was left at room temperature before loading on the gel.

For FLAG detection, 20 µg of total protein was run on 10% acrylamide SDS-PAGE (sodium dodecyl (lauryl) sulfate-polyacrylamide gel electrophoresis) gels and was then transferred to Immobilon-P PVDF membrane (EMD Millipore, Burlington, MA). Thereafter, the membrane was incubated with blocking buffer containing 1% bovine serum albumin (BSA) in 1× TBST (150 mM NaCl, 50 mM Tris, pH 7.5 + 0.05% Tween-20) for 1 h at room temperature with shaking, and was then incubated with 1/50,000 dilution in blocking buffer of monoclonal anti-FLAG M2 antibody (Sigma-Aldrich, Oakville, Ontario, Canada). Membranes were washed 3 times for 5 min each in TBST, then incubated with 1/50,000 dilution of horseradish peroxidase (HRP)-conjugated goat anti-mouse secondary antibody (Bio-Rad) for 1 h and washed 3 times for 5 min each in TBST. Membranes were then detected by using chemiluminescence reagent (Immobilon ECL reagents from Millipore, Sigma-Aldrich, Oakville, Ontario, Canada) and the amount of protein was quantified relative to total protein by using Coomassie blue staining of the membrane.

To analyze the expression of the FRQ protein, total protein was extracted from time-course samples with the same procedure as described, and 100 µg of total protein was run on 7.5% acrylamide SDS-PAGE gels. Proteins were transferred to PVDF membranes, which were stained with Ponceau Red and scanned before immunodetection. Blocking was conducted in 5% skimmed milk in TBS (150 mM NaCl, 50 mM Tris, pH 7.5), and anti-FRQ primary antibody incubation was done with a 1/20 dilution for 2 h at room temperature. The anti-FRQ antibody was generously supplied by A. Diernfellner and M. Brunner. The membrane was then washed 3 times with TBS for 5 min each time and incubated with HRP-conjugated goat anti-mouse secondary antibody diluted 1/10,000 in 5% milk/TBS at 4 °C overnight. The membranes were washed 3 times with TBS for 20 min each time at

room temperature and then detected using chemiluminescence reagent.

To quantify the relative amount of expressed protein, FRQ and GTR2 protein levels were normalized against total protein by staining the membrane with Ponceau Red before immunodetection or Coomassie Blue after immunodetection. Chemiluminescence was detected with a CCD camera and stained membranes were scanned. Pixel densities of both images were quantitated with ImageJ software. The ratio between the chemiluminescent signal and the intensity of total protein staining for that sample was defined as the relative expression level of the protein. When three biological replicates of time-courses were carried out, each time-course was normalized to itself by defining the mean expression level as 1.0. The three time-courses were then averaged to get the mean of the three independent experiments.

Co-immunoprecipitation and Mass Spectrometry Analysis

Co-immunoprecipitation (IP) was carried out using as bait either VTA-FLAG expressed from the ectopic *his-3* locus (*his-3⁺*::Native promoter-NCU05950::C-Gly::3xFLAG; *Δvta*) (Ratnayake et al., 2018) or GTR2-FLAG expressed from the endogenous locus as described above. Each experiment included an untagged control strain (*csp-1; chol-1 rasᵇᵈ*) and a strain expressing an unrelated FLAG-tagged protein, either NCU07839-FLAG expressed from the *his-3* locus (*his-3⁺*::Native promoter-NCU07839::C-Gly::3xFLAG) (Adhvaryu et al., 2016) or NCU08502-FLAG at the endogenous locus, constructed as for GTR2-FLAG. All strains carried the *csp-1; chol-1 rasᵇᵈ* background. Spores were inoculated on slants containing $1\times$ Vogel's salts, 2% glucose, 100 µM choline, and 2% agar, and were incubated at 30 °C in LL. After 7 days, spores were transferred into 100 mL liquid media containing Vogel's salts with 2% glucose and 100 µM choline, and were incubated at 25 °C with shaking at 150 r/min overnight in LL. These cultures were grown and harvested in constant light to minimize the amplitude of the circadian oscillator and remove circadian time as a variable in the results. Samples were harvested and were washed 3 times with phosphate-buffered saline (PBS; 10 mM phosphate, pH 7.4, 137 mM NaCl, 2.7 mM KCl) and distilled water on filter paper during vacuum filtration and were immediately frozen in liquid nitrogen and stored at −80 °C. Frozen samples were then ground in liquid nitrogen using a mortar and pestle, and were transferred to 500 µL of IP lysis buffer (50 mM HEPES, pH 7.5, 150 mM NaCl, 10% (v/v) glycerol, 0.02% (v/v) NP40, 1 mM EDTA, 1 mg/mL leupeptin, 1 mg/mL pepstatin A and 1 mM PMSF), and mixed by inversion for 20 s, left

at 4 °C for 5 min, and then centrifuged for 10 min at $15,130\times g$. Thereafter, supernatants were collected and 5 µL of the IP extracts was used to measure the protein concentration using the Bio-Rad DC Protein Assay.

Co-IP was carried out using 10 mg protein of the IP extracts. Protein extracts were first incubated with unconjugated beads to remove proteins that bind nonspecifically to the beads. 50 µL of Sepharose 4B beads (Sigma) was washed 3 times with the IP lysis buffer and was then incubated with 10 mg of protein. Samples were incubated at 4 °C with end-over-end agitation for 1 h. Samples were then centrifuged at $500\times g$ for 1 min and supernatant was collected.

Before using the antibody-conjugated beads for IP incubation, the beads were washed in buffer and glycine. 10 µL Anti-FLAG M2 Affinity Gel beads (Sigma-Aldrich) per sample was washed 3 times with IP lysis buffer at $500\times g$ at 4 °C and then incubated in 1 mL of 0.1 M glycine-HCl pH 3.5 buffer for 10 min. Beads were then washed another 3 times with IP lysis buffer and the supernatant was discarded. The washed beads were incubated with IP extract containing 10 mg of the protein overnight at 4 °C with end-over-end agitation. Samples were centrifuged at $750\times g$ for 1 min and beads were washed with the IP lysis buffer 3 times. Thereafter, the beads were washed for the final 2 times with FLAG rinsing buffer (50 mM NH_4HCO_3 pH8, 75 mM KCl, 2 mM Na_2EDTA). Frozen beads were sent to SPARC BioCentre (SickKids Proteomics, Analytics, Robotics & Chemical Biology Centre, Hospital for Sick Children, Toronto, Canada) for mass spectrometry analysis.

The results of mass spectrometry analysis were received as a Scaffold file (Scaffold 4.8.1—Proteome Software Inc., Portland, OR). Candidates were identified through the Uniprot database, and NCU numbers were identified by searching the *N. crassa* genome in FungiDB (Basenko et al., 2018). Proteins were identified as binding partners by the following criteria: Thresholds were set at 99% probability for protein identity and 95% for peptide identity. Proteins were included only if spectrum counts in the two control samples in each experiment were zero in all three independent experiments. Proteins found in the bait sample were included if they were present in at least two out of three experiments with at least two peptides identified in at least one experiment.

RESULTS

VTA and GTR2 Bind to Each Other and to Another Probable TOR Pathway Component

Our previous work (Ratnayake et al., 2018) identified VTA as a component of the TOR pathway in

Table 1.   Co-immunoprecipitation and mass spectrometry results.

Locus ID	Gene Product	MW (kDa)	Exp. 1		Exp. 2		Exp. 3		Total Counts
			Peptides	Counts	Peptides	Counts	Peptides	Counts	
Binding partners of VTA									
NCU00376	GTR2	48	3	9	9	13	12	16	38
NCU04811	Hypothetical protein	33	9	13	2	2	5	6	21
NCU01099	GTR1	45	2	2	3	3	6	6	11
NCU04376	Hypothetical protein	52	2	2	—	0	2	2	4
Binding partners of GTR2									
NCU04811	Hypothetical protein	33	1	5	2	4	2	3	12
NCU05950	VTA	17	3	4	—	0	2	2	6
NCU01099	GTR1	45	—	0	1	1	2	2	3

Binding partners of each FLAG-tagged bait protein are listed in descending order of total spectrum counts. An unrelated FLAG-tagged strain and a strain without any FLAG tag were used as controls in each experiment. NCU number represents the ID of the gene in the *N. crassa* genome database (FungiDB). Results are shown for three independent experiments.

Neurospora. To determine whether other components of this pathway also influence rhythmicity, we looked for binding partners of VTA that are likely to be TOR pathway components. Using our previously constructed VTA-FLAG fusion (Ratnayake et al., 2018), we carried out co-IP followed by mass spectrometry. Three independent experiments were carried out using an unrelated FLAG-tagged strain and a strain without any FLAG tag as controls in each experiment. Table 1 presents the results of the co-IPs. Proteins were only included in Table 1 if spectrum counts were zero in both control strains in all three experiments.

The top hit was gene NCU00376. This gene is identified in the *Neurospora* genome database FungiDB as guanine triphosphate binding-28 (*gtp-28*). Protein BLAST searches found that the closest homolog in *S. cerevisiae* is Gtr2p; one of the Ras-family GTPases found in the EGO complex that includes a homolog of VTA. We therefore refer to NCU00376 as *gtr2* and its product as GTR2. The closest homolog in mouse and human is RagD, a Ras-family GTPase found in the Ragulator-Rag GTPase complex. Both of these complexes function to transmit information about amino acid sufficiency to TOR.

The second-most frequent hit was gene NCU04811, identified in FungiDB as a hypothetical protein. Protein BLAST searches found homologs of NCU04811 in other closely related filamentous fungi but not in yeast or mammals, and no conserved protein domains were identified.

VTA-FLAG also co-precipitated NCU01099, identified in the *Neurospora* genome database as guanine triphosphate binding-6, *gtp-6*. Protein BLAST searches found that the closest homolog in yeast is Gtr1, and in mammals is RagB, components of the EGO and Ragulator complexes, respectively. We therefore propose identifying NCU01099 as *gtr-1*, and the product as GTR1, a probable component of the TOR pathway.

Protein NCU04376 was also found to co-precipitate with VTA-FLAG and is identified in FungiDB as a hypothetical protein, gene name *nup-23*. Homologs in closely related fungi with around 50%-60% identity indicate this protein may be related to nuclear pore proteins. A potential function in the TOR pathway has not been identified.

To confirm the association of VTA and GTR2 by reciprocal co-IP, we constructed a FLAG-tagged GTR2 using knock-in techniques to tag the endogenous gene. Race tube assays were carried out to confirm the normal function of the GTR2-FLAG protein and to ensure that the insertion of the FLAG tag did not disrupt the phenotype of the recipient strain. The banding phenotype, period, and growth rate of GTR2-FLAG were similar to the control on high choline (Figure 2, Table 2). The GTR2-FLAG strain on low choline displayed a long-period rhythm, as expected for choline-deprived wild-type strains, but the period was significantly shorter than the control, indicating some effect of the FLAG tag under these conditions. In the conditions of choline supplementation used in the co-IP experiments, the C-terminal FLAG tag did not disrupt the growth or significantly impair the clock-related functions of GTR2 protein.

As shown in Table 1, the uncharacterized protein NCU04811 was the top binding partner with GTR2-FLAG, and NCU05950 (VTA) was the second-most frequent binding partner, followed by GTR1. These results confirm the physical association between VTA and GTR2 and suggest a functional relationship between these proteins.

GTR2 Protein Levels Are Rhythmic

We previously reported that the level of the VTA protein is relatively constant with time and does not show significant rhythmicity (Ratnayake et al., 2018). Expression of VTA from a constitutive promoter rescues rhythmicity, demonstrating that expression of
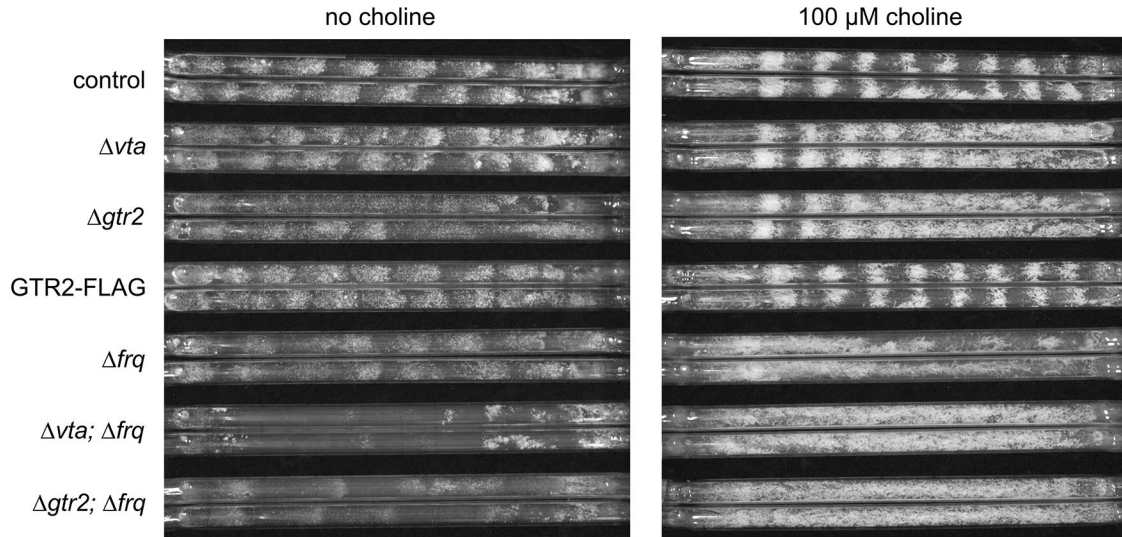
Figure 2. Effects of GTR2 deletion and FLAG tagging on free-running FRQ-less rhythms. Choline-requiring (*chol-1*) strains were grown on solid agar with or without 100 μM choline in race tubes in constant temperature and constant dark. Growth is from left to right. Two replicate tubes are shown for each strain. All strains carry the *csp-1*; *chol-1 ras^{bd}* genotype as well as deletions of *frq, vta*, or *gtr2*, or GTR2-FLAG knock-in, as indicated.

Table 2. Growth phenotypes of Δ*gtr2* and GTR2-FLAG strains.

Strain	No Choline		100 μM Choline	
	Period (h)	Growth Rate (mm/h)	Period (h)	Growth Rate (mm/h)
control	74.6 ± 3.32 (6)**	0.41 ± 0.01 (6)	21.0 ± 0.15 (6)	1.15 ± 0.01 (6)
Δ*vta*	73.5 ± 7.97 (6)**	0.40 ± 0.01 (6)	21.6 ± 0.14 (6)*	1.10 ± 0.01 (6)
Δ*gtr2*	NR	0.41 ± 0.02 (6)	22.0 ± 0.28 (6)**	1.03 ± 0.01 (6)
GTR2-FLAG	48.9 ± 3.35 (6)**†	0.48 ± 0.01 (6)	20.7 ± 0.09 (7)	1.16 ± 0.01 (7)
Δ*frq*	83.6 ± 4.73 (6)**	0.45 ± 0.01 (6)	NR	1.18 ± 0.01 (6)
Δ*vta; Δfrq*	NR	0.51 ± 0.01 (6)	NR	1.20 ± 0.01 (6)
Δ*gtr2; Δfrq*	NR	0.52 ± 0.05 (5)	NR	1.16 ± 0.01 (5)

Abbreviation: NR = not rhythmic. All strains carry the *csp-1; chol-1 ras^{bd}* genotype in addition to indicated genotypes. Data are reported as mean ± SEM (*N*) where *N* is the number of race tubes.
† Period on low choline is significantly different from control on low choline at *p* < 0.01.
*Period is significantly different from control on high choline at **p* < 0.05 or ***p* < 0.01.

the protein from its native promoter is not required for its clock function (Ratnayake et al., 2018). To compare the expression of the GTR2 protein to VTA, a time-course experiment was conducted using the GTR2-FLAG knock-in strain and an anti-FLAG antibody. Samples were harvested every 4 h across two circadian cycles from 24 to 72 h in darkness. Figure 3 demonstrates rhythmic expression of the protein. The peaks are at approximately 24-28, 48-52, and 68 h in darkness, which is close to the 21-22 h circadian period of *Neurospora* (Table 2). This low-amplitude rhythm is not obvious by visual inspection of the blots (Figure 3b) but is reproducibly found after quantitation (Figure 3a). A one-way analysis of variance (ANOVA) of the three replicate experiments found a significant effect of time, $p < 0.001$. Whether this rhythm is biologically significant remains to be determined. It has been reported that the RNA levels of GTR2 are rhythmic with a peak in the afternoon/evening at about 24 h in DD, or shortly after subjective dusk (Hurley et al., 2014). Assuming a period of about 21 h (Table 2), we would expect RNA peaks at about 24, 45, and 66 h in our culture system, a few hours before the protein peaks we observe (Figure 3a). GTR2 protein was also detected in a proteomics data set designed to identify rhythmic proteins (Hurley et al., 2018), although this data set failed to detect rhythmicity of the protein. This may be due to lower sensitivity of the proteomics method, or differences in the culture systems and growth media used.
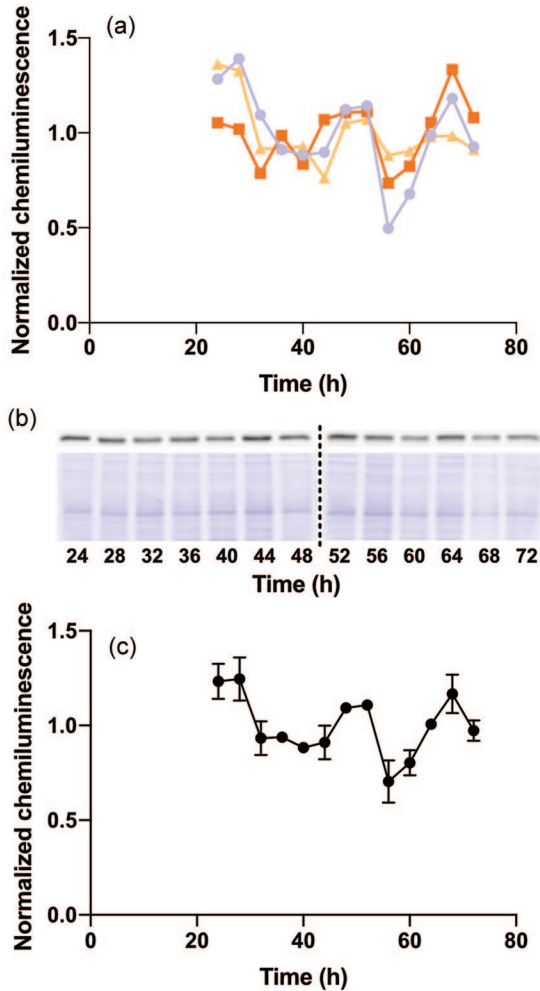
Figure 3. Rhythmic expression of GTR2 protein. (a) GTR2-FLAG (*csp-1; chol-1 ras^{bd}*) protein expression from three independent experiments across 24-72 h in constant conditions. (b) Immunoblot of one experiment showing GTR2-FLAG levels (above) and Coomassie blue staining (below). Dotted line indicates separation between two gels blotted to the same membrane. (c) Mean ± SEM from three independent experiments.

Figure 4. Expression of GTR2 protein in Δ*vta* background. (a) GTR2-FLAG (*csp-1; chol-1 ras^{bd}*; Δ*vta*) protein expression from three independent experiments across 24-72 h in constant conditions. Replicates were offset by +1.0 or +2.0 vertically for clarity. (b) Immunoblot of one experiment showing GTR2-FLAG levels (above) and Coomassie blue staining (below). Dotted line indicates separation between two gels blotted to the same membrane. (c) Mean ± SEM from three independent experiments.

VTA Is Essential to Maintain Rhythmicity of the GTR2 Protein

We next tested the hypothesis that the close physical association between VTA and GTR2 might affect the levels of GTR2 protein. To determine whether VTA protein is necessary to maintain the rhythmic expression of the GTR2 protein, three independent time-course experiments were conducted on a GTR2-FLAG strain in the absence of VTA. As shown in Figure 4, the rhythmicity of the protein was completely disrupted. Figure 4a shows that none of the three independent trials with the Δ*vta* strain show similarity with each other nor do they with the VTA wild type (Figure 3). A one-way
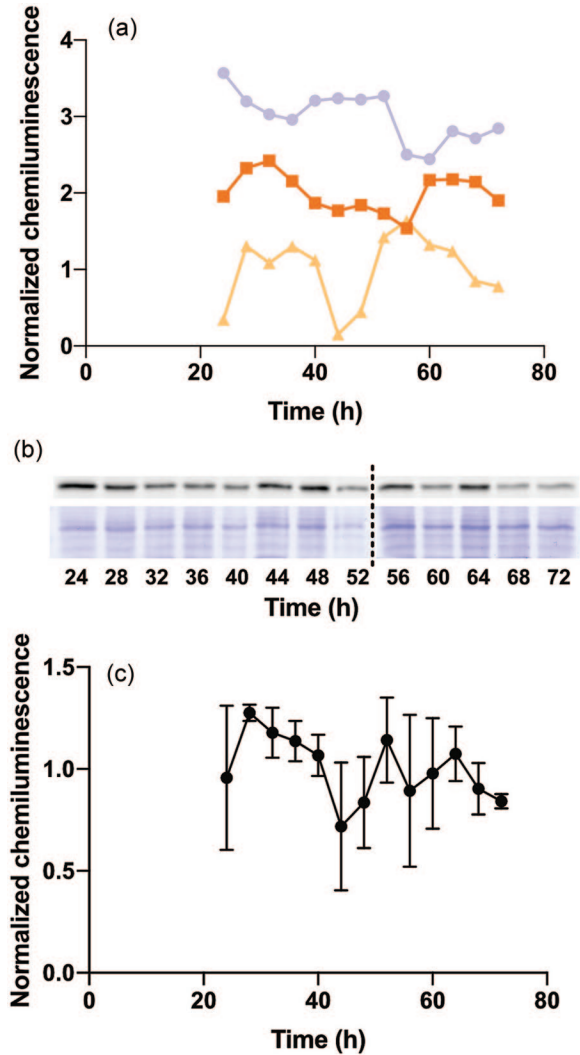
ANOVA of the three replicate experiments found no significant effect of time, $p > 0.5$.

To determine whether Δ*vta* changes the total amount of the GTR2 protein or just disrupts rhythmicity, one time point (28 h) was chosen which was at high levels in all experiments and three independent biological trials were loaded on the same gel, three samples of the wild type and three of Δ*vta* (data not shown). The relative amount of the GTR2 protein was quantified by calculating the ratio of chemiluminescence of each sample to its total protein by Coomassie staining. The mean of the three independent samples demonstrated similar ratios
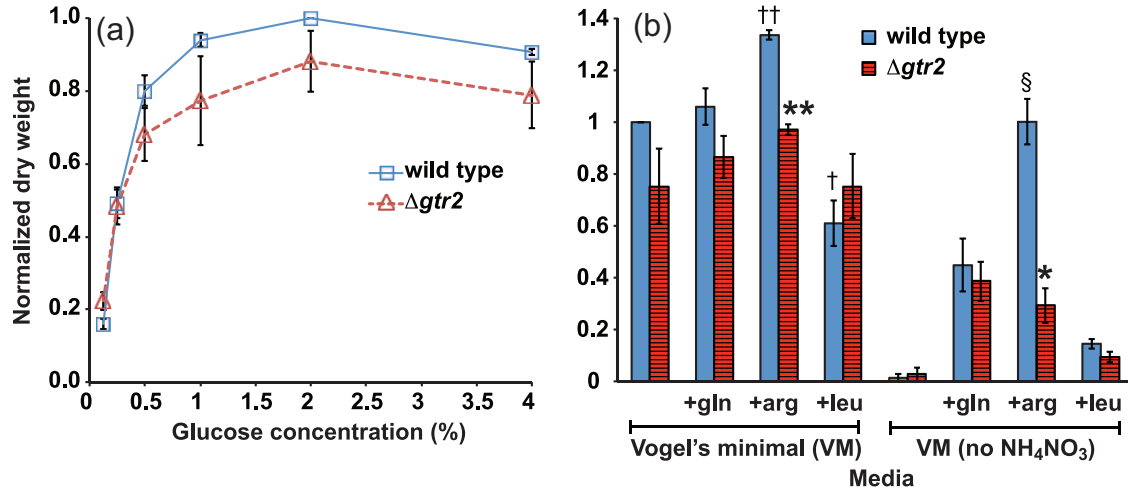
Figure 5. Growth response of Δ*gtr2* to nutritional states in liquid minimal media. Dry weights have been normalized such that wild type on VM + 2% glucose is equal to 1.0. (a) Effect of different glucose concentrations on the growth of Δ*gtr2* and *gtr2* wild-type strains. Error bars indicate mean ± SEM from four independent experiments. (b) Effect of adding different amino acids on the growth response of Δ*gtr2* and *gtr2* wild-type strains. Abbreviations: VM = Vogel's minimal medium. Error bars represent mean ± SEM from three independent experiments. [†]Amino acid supplement in VM significantly different from VM alone for the same strain, [†]$p < 0.05$ or [††]$p < 0.01$. [§]Arginine supplement significantly different from glutamine supplement in VM without NH_4NO_3 for the same strain, $p < 0.05$ (§). *Δ*gtr2* significantly different from wild type on the same growth medium, *$p < 0.05$ or **$p < 0.01$.

of 0.94 ± 0.08 (SEM) for GTR2-FLAG (*csp-1; chol-1 ras^bd^*) and 0.82 ± 0.20 (SEM) for GTR2-FLAG (*csp-1; chol-1 ras^bd^*; Δ*vta*). A paired two-tailed Student's *t* test gave a *p* value of 0.65, indicating that the difference is not statistically significant. It can be concluded that VTA protein does not control the total level of expression of GTR2 protein, but that the presence of VTA is required to maintain rhythmic expression of GTR2 protein.

GTR2 Deletion Disrupts Nutrient Sensing for Growth

If GTR2 is a component of the nutrient-sensing TOR pathway in *Neurospora*, we predicted that deletion of *gtr2* should affect growth responses to varied nutritional conditions, as seen in Δ*vta* (Ratnayake et al., 2018). We obtained the deletion of NCU00376 (Δ*gtr2*) from FGSC and compared its growth to the wild-type Oak Ridge strain. Both strains were grown in liquid media to allow easy harvesting and measurement of dry weight, and growth in response to varied concentrations of glucose (Figure 5a) as well as varied amino acid supplementation (Figure 5b) was assayed. We previously reported (Ratnayake et al., 2018) that the growth of the Δ*vta* strain did not respond to increased glucose concentration as strongly as the wild type. The effects of glucose on the Δ*gtr2* strain trended in the same direction (Figure 5a), although the differences between Δ*gtr2* and wild type did not reach statistical significance.

In response to amino acids, the Δ*gtr2* strain differed from wild type. When amino acids were added to nitrogen-containing Vogel's minimal medium (VM; Figure 5b), growth of the wild-type strain was significantly increased by arginine and decreased by leucine but was not significantly affected by glutamine when compared to VM alone. Growth of the Δ*gtr2* strain on nitrogen-containing VM failed to respond significantly to any of the amino acids (Figure 5b). When the two strains were compared to each other on the same VM media, the growth of Δ*gtr2* was significantly different from wild type only on arginine-supplemented VM (Figure 5b). As expected, neither strain could grow significantly on VM without an added nitrogen source. Glutamine could be utilized as sole nitrogen source in the absence of NH_4NO_3 equally well by both strains (Figure 5b). When comparing glutamine to arginine in VM without NH_4NO_3, the wild type responded significantly more to arginine than glutamine but the Δ*gtr2* strain did not. When the two strains were compared to each other on the same VM media without NH_4NO_3, the growth of Δ*gtr2* was significantly different from wild type only on arginine-supplemented medium (Figure 5b). Neither strain used leucine efficiently as sole carbon source. We conclude that the response of Δ*gtr2* to varied nutritional conditions is consistent with our identification of GTR2 as a component of the amino acid–sensing complex of the TOR pathway.

GTR2 Deletion Disrupts Free-Running FRQ-Less Rhythms and Entrainment to Heat Pulses

Having identified GTR2 as a binding partner of VTA and a component of the TOR pathway, we tested the hypothesis that GTR2, like VTA, is required to maintain FRQ-less rhythmicity. The Δgtr2 deletion was crossed into our laboratory strains to assay clock phenotypes. FRQ-less rhythmicity can be revealed by growing choline-requiring chol-1 strains on media without added choline, and this rhythmicity continues in frq-null strains (Lakin-Thomas and Brody, 2000). Choline-requiring strains carrying deletions of gtr2, vta, and/or frq were grown on solid agar medium in conditions of constant temperature and constant darkness to assay free-running conidiation rhythms. As shown in Figure 2 and Table 2, long-period rhythmicity can be seen in both the control and Δfrq strains without choline but rhythmicity in Δfrq strains is disrupted when either vta or gtr2 is also deleted.

On choline-containing medium, both Δvta and Δgtr2 are rhythmic in a frq+ background but with a low-amplitude dampened rhythm (Figure 2). In experiments without choline, the phenotype of Δvta (in the frq+ background) is variable, displaying rhythmicity in some instances (as in Figure 2) and not in others. The Δgtr2 phenotype can also display infrequent banding in the frq+ background without choline (comparing the two representative cultures in Figure 2). In contrast, the phenotypes of both Δvta and Δgtr2 in the Δfrq background never display regular banding patterns or resemble control strains, either with or without choline. These results are consistent with the hypothesis that a weak oscillator is operating in the Δvta and Δgtr2 strains on media both with and without choline in the frq+ background. This oscillator would require a functional frq gene, as seen by disrupted rhythmicity in the Δvta and Δgtr2 strains in the Δfrq background. It appears, therefore, that both the FLO in Δfrq strains and the frq-based oscillator in frq+ strains require VTA and GTR2 for robust rhythmicity.

A second assay for FRQ-less rhythmicity depends on the behavior of circadian oscillators when entrained to repeated cycles (T-cycles) of short heat pulses. The entrained peak shape and timing change with the length of the T-cycle for an entrained oscillator, and this behavior in Δfrq strains provides evidence for the existence of an entrainable oscillator in the absence of a functional frq gene (Lakin-Thomas, 2006a; Merrow et al., 1999; Roenneberg et al., 2005). FRQ-deleted Δgtr2 and Δvta strains were compared to the Δfrq control in T-cycles of 2 h heat pulses at intervals of 20 or 24 h and the conidiation density profiles for an average cycle were compared (Figure 6). As shown previously (Ratnayake et al., 2018), Δvta entrains with a phase several hours earlier than the

control (Figure 6a) and the timing and peak shape of Δvta do not change with the T-cycle, unlike the Δfrq control (Figure 6b). The behavior of Δgtr2 is very similar to Δvta (Figure 6a and 6b), suggesting they may function in a similar way to disrupt the FLO.

GTR2 Is Essential to Maintain Expression Level and Rhythmicity of the FRQ Protein

We have previously shown that functional VTA is required to maintain the normal molecular rhythm of the FRQ protein (Ratnayake et al., 2018). We therefore tested the hypothesis that GTR2, like VTA, is also required for normal FRQ rhythmicity. To first confirm that the FRQ/WCC TTFL is functional in our time-course samples, immunoblotting with anti-FRQ antibody was conducted on the same biological samples as in Figure 3, and FRQ protein demonstrated the expected rhythm in protein amount and phosphorylation state across two circadian cycles in the GTR2 wild-type strain, GTR2-FLAG (csp-1; chol-1 ras^{bd}; Figure 7). A one-way ANOVA of the three replicate experiments found a significant effect of time on protein levels, $p < 0.001$. To determine whether GTR2 is essential for the rhythm of FRQ protein, another time-course experiment was conducted on a Δgtr2 (csp-1; chol-1 ras^{bd}) strain. It was found that the FRQ protein level was rhythmic but appeared to dampen over time (Figure 8). A one-way ANOVA of the three replicate experiments found a significant effect of time on protein levels, $p < 0.001$.

To quantitate the effect of the absence of GTR2 on the total level of expression of FRQ, we re-ran selected GTR2 wild type and Δgtr2 protein samples and blotted the two gels on one membrane for immunodetection with anti-FRQ antibody and direct comparison of FRQ protein levels. Three time points were chosen near the peaks of expression at 24, 44, and 60 h. The membrane was stained with Ponceau Red before immunodetection and the relative amount of the FRQ protein in each lane was calculated relative to total protein in that lane. The results indicated that in the absence of GTR2 protein, the expression level of the FRQ protein tends to be lower than GTR2 wild type and is significantly lower at the third time point (Figure 9). We conclude that the presence of GTR2 is essential for normal FRQ expression levels, and the rhythm of FRQ protein levels damps out in the absence of GTR2.

DISCUSSION

The results reported here add to our understanding of the structure and function of the TOR pathway in *Neurospora*. In addition to our previous identification of NCU05950 as VTA, homologous to
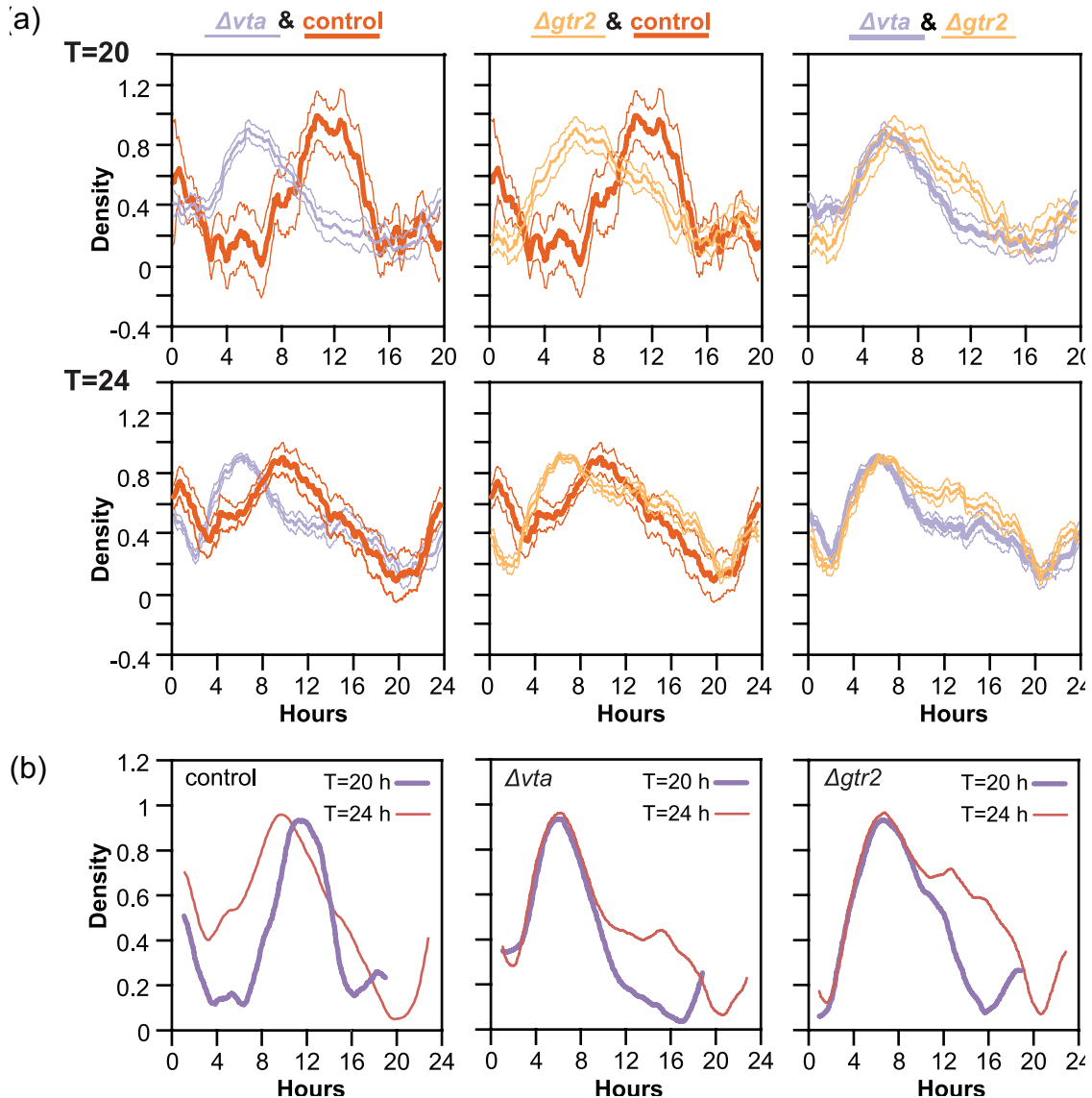
Figure 6.   Effects of GTR2 deletion on entrainment of the FLO to cycles of heat pulses. FRQ-less strains (Δfrq) were grown on solid agar in race tubes in DD and entrained to repeated cycles of 2 h heat pulses (22 °C > 32 °C) at intervals of $T = 20$ h or $T = 24$ h. All strains carry the *csp-1; chol-1 ras^{bd}; Δfrq* genotype as well as deletions of *vta* or *gtr2*. Density of conidiation was averaged over 4-6 race tubes and the density profile for an average entrained cycle was normalized to peak = 1.0. Normalized conidiation density profiles are plotted against hours after the beginning of the heat pulse. (a) Control and deletion strains are compared to each other for two *T*-cycles, $T = 20$ h and $T = 24$ h. Thin lines are ±1 SEM. (b) Density profiles were smoothed with a 19-point running average to identify the peak times and plots for $T = 20$ (thick lines) and $T = 24$ (thin lines) are compared for each strain.

Ego1 in yeast and LAMTOR1 in mammals, we have now identified the product of NCU00376 as GTR2, homologous to one of the Rag GTPases found in the amino acid–sensing complexes of yeast and mammalian TOR pathways. We also tentatively identify the product of NCU01099 as GTR1, another Rag GTPase in the same complex as VTA and GTR2, and we have demonstrated that these proteins can be found in a complex.

Our nutritional experiments with VTA and GTR2 have focused attention on arginine as a potential signal for activating growth response through the TOR signaling pathway in *Neurospora*. This raises interesting points of difference with the mammalian and yeast amino acid–sensing pathways. Glutamine is most effective in activating the yeast TORC1, while leucine and arginine are most effective for activation of mammalian TORC1 (Boutouja et al., 2019). In contrast, *Neurospora* growth is inhibited by leucine, not activated, and growth does not respond to added glutamine in the presence of another nitrogen source (Figure 5b). The activation of growth by arginine, and
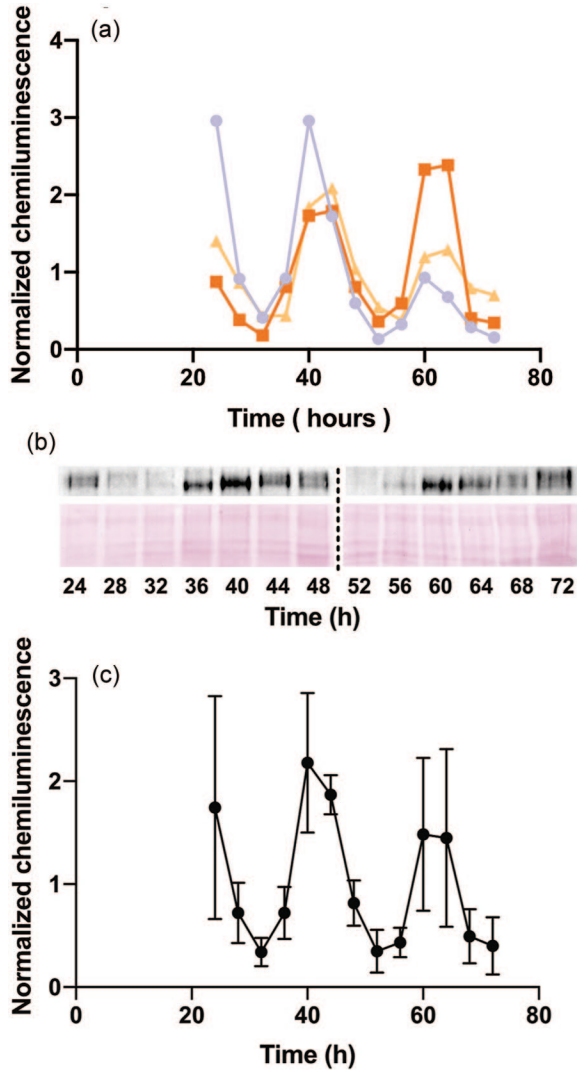
Figure 7.   FRQ protein levels in the presence of GTR protein. (a) FRQ (*csp-1; chol-1 ras*^{bd}) protein expression from three independent experiments across 24-72 h in constant conditions. (b) Immunoblot of one experiment showing rhythm of FRQ levels (above) and Ponceau Red staining (below). Dotted line indicates separation between two gels blotted to the same membrane. (c) Mean ± SEM from three independent experiments.

Figure 8.   FRQ protein levels in the absence of GTR2 protein. (a) FRQ (*csp-1; chol-1 ras*^{bd}; Δ*gtr2*) protein expression from three independent experiments across 24-72 h in constant conditions. (b) Immunoblot of one experiment showing rhythm of FRQ levels (above) and Ponceau Red staining (below). Dotted line indicates separation between two gels blotted to the same membrane. (c) Mean ± SEM from three independent experiments.

the lack of effect of arginine in the Δ*gtr2* strain, may be related to the role of arginine in *Neurospora* as a storage compound in vacuoles, releasing its nitrogen when glutamine is depleted (Legerton and Weiss, 1984). It has been proposed that amino acids in mammalian lysosomes may activate TOR through an "inside-out" mechanism, signaling to the cytoplasmic TOR complex through lysosomal transporters (González and Hall, 2017).

Over the last decade, there has been increasing interest in identifying the links between circadian rhythms and metabolism. There is substantial evidence for the existence of metabolic oscillators that
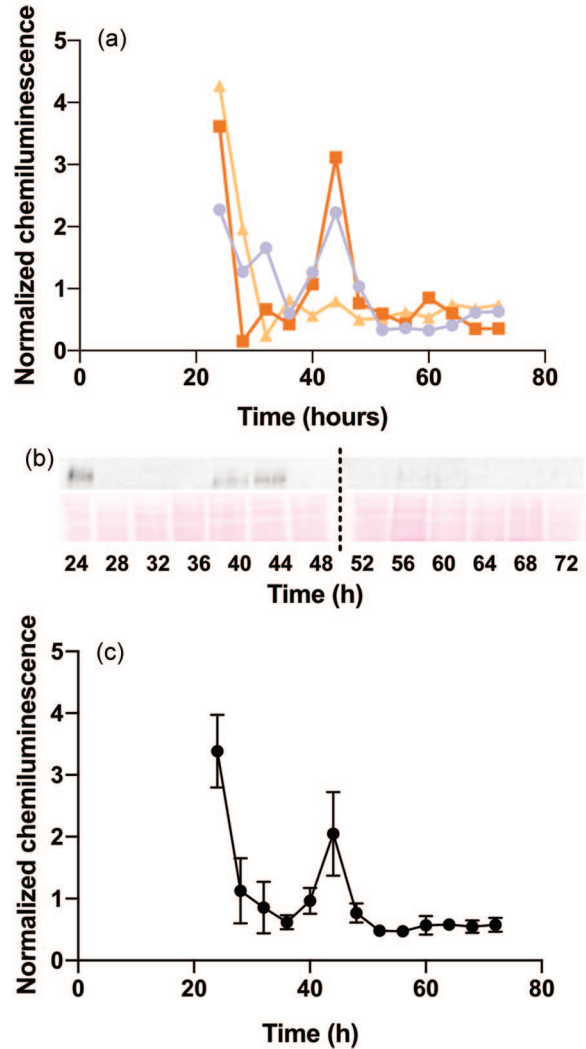
might be present in addition to the TTFL. One potential biochemical link between these two is the TOR signaling pathway (Lakin-Thomas, 2019). TOR signaling has been linked to circadian clocks in several organisms (Lakin-Thomas, 2019), both as an output pathway and in a more direct role in generating or maintaining rhythmicity. Evidence for these more direct effects of TOR on clocks comes from studies on *Drosophila* (Zheng and Sehgal, 2010), human cell lines (Feeney et al., 2016; Walton et al., 2018), and both SCN and peripheral tissues of mice (Cao, 2018; Lipton et al., 2017). In recent studies on *Arabidopsis*, TOR was found to be essential for glucose- and nicotinamide-mediated control of the circadian period (Zhang
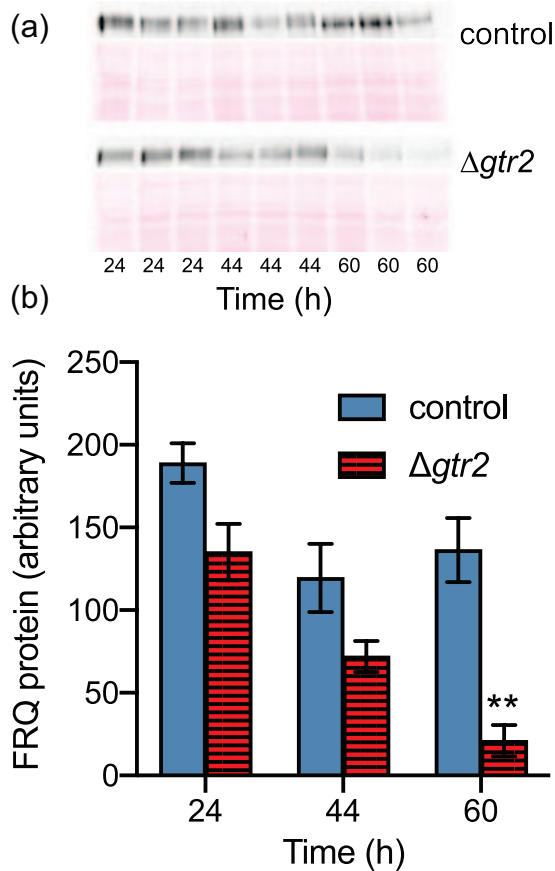
Figure 9. FRQ protein levels in the presence and absence of GTR2. 24, 44, and 60 h samples were chosen to compare the total amount of FRQ protein between strains. (a) Immunoblot showing FRQ protein (above) and Ponceau Red staining (below) for control (*csp-1; chol-1 ras^bd^*) and GTR2 deletion (*csp-1; Δgtr2; chol-1 ras^bd^*) with three replicates for each time point. Two gels were blotted to the same membrane for immunodetection. (b) Mean ± SEM from three independent samples for each strain. **Control significantly different from Δgtr2, $p < 0.001$.

interaction of these TOR pathway components with the FRQ/WCC TTFL. Our previous results demonstrated that the FRQ protein rhythm dampens over time in the absence of VTA protein (Ratnayake et al., 2018). In our current work with GTR2, similar results were obtained, and the presence of GTR2 was shown to be essential to maintain normal expression of the FRQ protein. In related research (Diernfellner et al., 2019), the clock-controlled gene *prd-4* was found to be essential for FRQ phosphorylation in response to translation inhibition. This phosphorylation requires an upstream kinase of PRD-4, which was identified as TORC1 using phosphorylation of S6 as an assay for TORC1 activity (Diernfellner et al., 2019). We have not characterized the pathway through which VTA and GTR2 affect FRQ, but our work is consistent with the work of Diernfellner et al. and suggests a pathway: VTA > GTR2 > TOR > PRD4 > FRQ.

Overall, it can be concluded that the presence of both VTA and GTR2 is necessary for the normal function of FRQ and the circadian system, demonstrating a strong connection between the TOR pathway and circadian rhythms. We propose that GTR2 and VTA maintain circadian rhythmicity through the complementary interaction of a FLO with the FRQ/WCC TTFL, supporting our model that the TTFL is not adequate to explain circadian rhythms in *N. crassa*. We hypothesize that FLO may work through the TOR pathway, which is an essential metabolic signaling pathway in all eukaryotes. Our results are expected to have implications for enhancing the understanding of the circadian systems of other organisms, and for understanding the fundamentally important process of timekeeping in eukaryotes.

et al., 2019), and knocking down TOR activity with inhibtors, micro-RNA or RNAi was found to lengthen the circadian period (Wang et al., 2020).

Our previous work (Ratnayake et al., 2018) demonstrated that deletion of *vta* dampens conidiation rhythmicity in FRQ wild-type strains and abolishes FRQ-less rhythms. These results provided evidence of a role for the TOR pathway in rhythmicity of *Neurospora* in the presence or absence of a functional FRQ/WCC TTFL. In our current work with the GTR2 deletion, similar results were obtained from assays of conidiation rhythmicity including assays for the presence of a FLO. This directs attention to questions about the roles of VTA and GTR2 in the circadian system and whether VTA and GTR2 function in the same pathway to maintain circadian rhythms.

Time-course experiments with the anti-FRQ antibody have revealed interesting insights into the

CONFLICT OF INTEREST STATEMENT

The author(s) have no potential conflicts of interest with respect to the research, authorship, and/or publication of this article.

ORCID iDs

Rosa Eskandari https://orcid.org/0000-0002-5641-1699

Patricia L. Lakin-Thomas https://orcid.org/0000-0002-0545-9561

REFERENCES

Adhvaryu K, Firoozi G, Motavaze K, and Lakin-Thomas P (2016) PRD-1, a component of the circadian system of *Neurospora crassa*, is a member of the DEAD-box RNA helicase family. J Biol Rhythms 31:258-271.

Basenko EY, Pulman JA, Shanmugasundram A, Harb OS, Crouch K, Starns D, Warrenfeltz S, Aurrecoechea C, Stoeckert CJ, Kissinger JC, et al. (2018) FungiDB: an integrated bioinformatic resource for fungi and oomycetes. J Fungi 4:1-28.

Bass J (2012) Circadian topology of metabolism. Nature 491:348-356.

Boutouja F, Stiehm C, and Platta H (2019) mTOR: a cellular regulator interface in health and disease. Cells 8:18.

Cao R (2018) mTOR signaling, translational control, and the circadian clock. Front Genet 9:1-10.

Diernfellner ACR, Lauinger L, Shostak A, and Brunner M (2019) A pathway linking translation stress to checkpoint kinase 2 signaling in *Neurospora crassa*. Proc Natl Acad Sci U S A 116:17271-17279.

Dunlap JC, Ringelberg C, Litvinkova L, Colot HV, Turner GE, Park G, Crew CM, Borkovich KA, and Weiss RL (2006) A high-throughput gene knockout procedure for *Neurospora* reveals functions for multiple transcription factors. Proc Natl Acad Sci 103:10352-10357.

Feeney KA, Hansen LL, Putker M, Olivares-Yañez C, Day J, Eades LJ, Larrondo LF, Hoyle NP, O'Neill JS, and Van Ooijen G (2016) Daily magnesium fluxes regulate cellular timekeeping and energy balance. Nature 532:375-379.

González A and Hall MN (2017) Nutrient sensing and TOR signaling in yeast and mammals. EMBO J 36:397-408.

Honda S and Selker EU (2009) Tools for fungal proteomics: multifunctional *Neurospora* vectors for gene replacement, protein expression and protein purification. Genetics 182:11-23.

Hurley JM, Dasgupta A, Emerson JM, Zhou X, Ringelberg CS, Knabe N, Lipzen AM, Lindquist EA, Daum CG, Barry KW, et al. (2014) Analysis of clock-regulated genes in *Neurospora* reveals widespread posttranscriptional control of metabolic potential. Proc Natl Acad Sci U S A 111:16995-17002.

Hurley JM, Jankowski MS, De los Santos H, Crowell AM, Fordyce SB, Zucker JD, Kumar N, Purvine SO, Robinson EW, Shukla A, et al. (2018) Circadian proteomic analysis uncovers mechanisms of post-transcriptional regulation in metabolic pathways. Cell Syst 7:613-626.e5.

Jewell JL, Russell RC, and Guan K (2013) Amino acid signalling upstream of mTOR. Nat Rev Mol Cell Biol 14:133-139.

Lakin-Thomas PL (2006a) Circadian clock genes *frequency* and *white collar-1* are not essential for entrainment to temperature cycles in *Neurospora crassa*. Proc Natl Acad Sci U S A 103:4469-4474.

Lakin-Thomas PL (2006b) Transcriptional feedback oscillators: maybe, maybe not . . . J Biol Rhythms 21:83-92.

Lakin-Thomas PL (2019) Circadian rhythms, metabolic oscillators, and the target of rapamycin (TOR) pathway: the *Neurospora* connection. Curr Genet 65:339-349.

Lakin-Thomas PL and Brody S (2000) Circadian rhythms in *Neurospora crassa*: lipid deficiencies restore robust rhythmicity to null *frequency* and *white-collar* mutants. Proc Natl Acad Sci U S A 97:256-261.

Lakin-Thomas PL, Bell-Pedersen D, and Brody S (2011) The genetics of circadian rhythms in *Neurospora*. In: Brody S, editor. *The Genetics of Circadian Rhythms*. Amsterdam (the Netherlands): Elsevier. p. 55-104.

Legerton TL and Weiss RL (1984) Mobilization of vacuolar arginine in *Neurospora crassa*. J Biol Chem 259:8875-8879.

Li S and Lakin-Thomas PL (2010) Effects of *prd* circadian clock mutations on FRQ-less rhythms in *Neurospora*. J Biol Rhythms 25:71-80.

Li S, Motavaze K, Kafes E, Suntharalingam S, and Lakin-Thomas PL (2011) A new mutation affecting FRQ-less rhythms in the circadian system of *Neurospora crassa*. PLoS Genet 7:e1002151.

Lipton JO, Boyle LM, Yuan ED, Hochstrasser KJ, Chifamba FF, Nathan A, Tsai PT, Davis F, and Sahin M (2017) Aberrant proteostasis of BMAL1 underlies circadian abnormalities in a paradigmatic mTOR-opathy. Cell Rep 20:868-880.

Loewith R and Hall MN (2011) Target of rapamycin (TOR) in nutrient signaling and growth control. Genetics 189:1177-1201.

McCluskey K, Wiest A, and Plamann M (2010) The Fungal Genetics Stock Center: a repository for 50 years of fungal genetics research. J Biosci 35:119-126.

Merrow M, Brunner M, and Roenneberg T (1999) Assignment of circadian function for the *Neurospora* clock gene frequency. Nature 399:584-586.

Nakajima M, Imai K, Ito H, Nishiwaki T, Murayama Y, Iwasaki H, Oyarna T, and Kondo T (2005) Reconstitution of circadian oscillation of cyanobacterial KaiC phosphorylation in vitro. Science 308:414-415.

Oldenburg KR, Vo KT, Michaelis S, and Paddon C (1997) Recombination-mediated PCR-directed plasmid construction in vivo in yeast. Nucleic Acids Res 25:451-452.

Park G, Servin JA, Turner GE, Altamirano L, Colot HV, Collopy P, Litvinkova L, Li L, Jones CA, Diala FG, et al. (2011) Global analysis of serine-threonine protein kinase genes in *Neurospora crassa*. Eukaryotic Cell 10:1553-1564.

Pinto D, Duarte M, Soares S, Tropschug M, and Videira A (2008) Identification of all FK506-binding proteins from *Neurospora crassa*. Fungal Genet Biol 45:1600-1607.

Powis K, Zhang T, Panchaud N, Wang R, De Virgilio C, and Ding J (2015) Crystal structure of the Ego1-Ego2-Ego3 complex and its role in promoting Rag GTPase-dependent TORC1 signaling. Cell Res 25:1043-1059.

Ratnayake L, Adhvaryu KK, Kafes E, Motavaze K, and Lakin-Thomas PL (2018) A component of the TOR (Target of Rapamycin) nutrient-sensing pathway plays a role in circadian rhythmicity in *Neurospora crassa*. PLoS Genet 14:e1007457.

Roenneberg T, Dragovic Z, and Merrow M (2005) Demasking biological oscillators: properties and principles of entrainment exemplified by the *Neurospora* circadian clock. Proc Natl Acad Sci U S A 102:7742-7747.

Sancak Y, Bar-Peled L, Zoncu R, Markhard AL, Nada S, and Sabatini DM (2010) Ragulator-rag complex targets mTORC1 to the lysosomal surface and is necessary for its activation by amino acids. Cell 141:290-303.

Saxton RA and Sabatini DM (2017) mTOR signaling in growth, metabolism, and disease. Cell 168:960-976.

Shertz CA, Bastidas RJ, Li W, Heitman J, and Cardenas ME (2010) Conservation, duplication, and loss of the Tor signaling pathway in the fungal kingdom. BMC Genomics 11:510.

Tseng R, Goularte NF, Chavan A, Luu J, Cohen SE, Chang YG, Heisler J, Li S, Michael AK, Tripathi S, et al. (2017) Structural basis of the day-night transition in a bacterial circadian clock. Science 355:1174-1180.

van Ooijen G and Millar AJ (2012) Non-transcriptional oscillators in circadian timekeeping. Trends Biochem Sci 37:484-492.

Walton ZE, Patel CH, Brooks RC, Yu Y, Ibrahim-Hashim A, Riddle M, Porcu A, Jiang T, Ecker BL, Tameire F, et al. (2018) Acid suspends the circadian clock in hypoxia through inhibition of mTOR. Cell 174:72-87.

Wang Y, Qin Y, Li B, Zhang Y, and Wang L (2020) Attenuated TOR signaling lengthens circadian period in *Arabidopsis*. Plant Signal Behav 15:1710935.

Yonehara R, Nada S, Nakai T, Nakai M, Kitamura A, Ogawa A, Nakatsumi H, Nakayama KI, Li S, Standley DM, et al. (2017) Structural basis for the assembly of the Ragulator-Rag GTPase complex. Nat Commun 8:1625.

Zhang N, Meng Y, Li X, Zhou Y, Ma L, Fu L, Schwarzländer M, Liu H, and Xiong Y (2019) Metabolite-mediated TOR signaling regulates the circadian clock in *Arabidopsis*. Proc Natl Acad Sci U S A 116:25395-25397.

Zheng X and Sehgal A (2010) AKT and TOR signaling set the pace of the circadian pacemaker. Curr Biol 20:1203-1208.